U P W A S H A N D S I D E W A S H I N D U C E D B Y C E R T A I N C O N T R O L S U R F A C E S I N A S U P E R S O N I C F L O W

Thesis by

Ernest I. Pritchard

In Partial Fulfillment of the Requirements

For the Degree of

Aeronautical Engineer

California Institute of Technology

Pasadena, California

1948

ACKNOWLEDGEMENT

The author wishes to thank Dr. Paco Lagerstrom for his guidance and the ideas which he contributed to assist in the preparation of this thesis.

My sincere thanks also to Dr. Paco Lagerstrom, Dr. H. J. Stewart, and Dr. Charles DePrima for their reviews of, and suggestions on the manuscript.

SUMMARY

Dr. Lagerstrom's development of the conical flow theory to apply to upwash and sidewash problems (see reference 1) has been applied to the case of a deflected roll control surface. The upwash behind, and in the plane of, the deflected control surface at 0, 1, 4, and 9 chord lengths behind the wing is calculated. The whole upwash-sidewash field, an infinite distance downstream of the control surface, (in the Trefftz plane), is also calculated. It is shown that a rolling moment is induced on any aerodynamic surface - vertical, horizontal, or oblique - that lies in the wake of the deflected control surface. This induced rolling moment is in the reverse direction of that prescribed by the deflection of the roll control surface. One simple case is cited where the magnitude of the induced rolling moment is larger than that produced directly by the roll control surface, thus causing a reversal of the roll direction. An induced yawing moment may also be encountered if a vertical aerodynamic surface, not symmetrical with respect to the plane of the wing, is present in the wake of the deflected control surface.

TABLE OF CONTENTS

LIST OF FIGURES

NOTATION

The coordinates used are illustrated on the right. x_1, x_3 is the plane in which the wing is considered to be located in the linearized conical flow theory. x_3 lies in the direction of the velocity from infinity. u_1, u_2, and u_3 are the perturbation velocities in the x_1, x_2 and x_3 directions respectively.

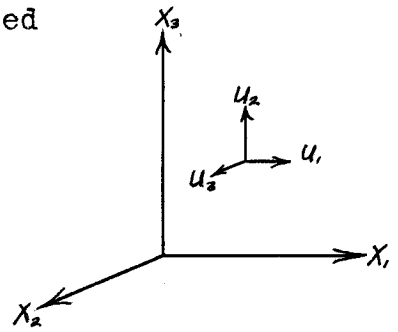

Other symbols are:

$b = \frac{x_1}{m x_3}$ (denotes position of side edge of wing)

$B = \frac{1-\sqrt{1-b^2}}{b}$

c = chord of the wing

c_p = pressure coefficient $= \frac{p - p_\infty}{\frac{\rho_\infty}{2} U_\infty^2}$

$m = \frac{1}{\sqrt{M^2-1}} = \tan \mu$

M = free stream Mach number

Q - denotes a point in the wake of the wing

$t = \frac{x_1}{m x_3}$ = usual conical flow coordinate in the plane of the wing

$T = \frac{1-\sqrt{1-t^2}}{t}$

$t^* = \frac{\frac{x_1}{mc} - b}{\frac{x_3}{c} - 1}$

$T^* = \frac{1-\sqrt{1-t^{*2}}}{t^*}$

U_∞ = free stream velocity

u_1 = sidewash

u_2 = upwash

u_3 = perturbation velocity in the free stream direction

$z = x_1 + ix_2 = r_1 e^{i\theta_1}$ = complex variable in Trefftz plane

α = angle of attack

$\zeta = x + iy = Re^{i\theta}$ = complex variable in the ζ plane

μ = Mach angle = arc tan m

A. INTRODUCTION

The work in this thesis was done jointly by Mr. Welko E. Gasich and myself. The results are being reported individually as required by the California Institute of Technology.

Missiles flying at supersonic speeds have been observed to roll in the opposite direction from that prescribed by the deflection of the roll control surfaces. The cause of this roll reversal was unknown. One possible explanation was the effect that the upwash-sidewash field would have on the aerodynamic surfaces downstream of the roll control surface. This effect was unknown and it is the purpose of this report to present the upwash and sidewash data necessary for calculating this induced rolling moment for any given configuration. These data are also useful for stability calculations.

The linearized conical flow methods of reference (1) are directly applicable to the problem at hand. The method makes use of the linearizing approximations of the small perturbation theory. Therefore, the results are applicable only for small angles of attack and the usual Mach number limitations. These limitations are determined by the accuracy desired in the results. The methods used in this thesis apply only to control surfaces which have no twist and whose profiles are symmetrical about a straight mean camber line. No attempt has been made in this report to take into account the presence of a fuselage or other body.

The amount of error in assuming no wing body interference is not known.

As in all applications of the linearized theory, the problem may be divided into the thickness case and the case of the flat plate at an angle of attack. The solutions to these two cases are then superimposed. It is obvious that the thickness case does not contribute to the upwash-sidewash field behind the control surface. Therefore, only the case of the flat plate at an angle of attack is considered here. In the derivation of the formulas used, the wing, or control surface is considered to lie in a horizontal plane. The boundary conditions on the wing are applied in this horizontal plane in the usual manner for the linearized theory. This horizontal plane is sometimes referred to as the plane of the wing.

The derivation of the basic methods used in this thesis are found in reference (1) and not repeated here. The application of these formulas to this particular upwash and sidewash problem are discussed, and the results presented in graphical form at the end of the thesis.

The upwash-sidewash field downstream of finite deflected control surfaces, such as are pictured in Figure (I), is obtained by the principle of superposition. It is well known that in first order theory there is no sidewash or downwash (reference 2) behind a two dimensional wing in a supersonic stream. Therefore, sections II and IV of the wing in Figure (I) do not contribute to the downstream sidewash-upwash field. The solutions for the upwash in the plane of the wing at finite distances behind it and in the Trefftz plane

are plotted for rectangular and trapezoidal wing tips (section I and V) in reference (1). Formulas for the sidewash behind the wing due to sections I and V are also given, but the calculations have not been carried out to the author's knowledge. Thus the only unknown contribution to the trailing upwash-sidewash field comes from the Mach cone arising from the discontinuity in angle of attack, which is section III in Figure (I). This discontinuity in angle of attack also arises in the case where the roll control surface is a section of a fixed wing. The solution may be superimposed in this case or any other, where a discontinuity in angle of attack is involved, within the restrictions of the theory. The leakage of air through the wing at the discontinuity will be neglected. There is a certain amount of justification for this, since control surface slits are often sealed.

Thus the problem is reduced to finding the downstream sidewash-upwash field behind a wing of infinite span with a discontinuity in angle of attack of $2\alpha_0$ (see Figure II). We again remind the reader that a two dimensional wing makes no contribution to the trailing upwash and sidewash. If a two dimensional wing of angle of attack $-\alpha_0$ were superimposed on the deflected control surface of infinite span pictured in Figure (II), the trailing upwash-sidewash field would not be affected. The discontinuity in angle of attack for the combination would remain the same, but the angle of attack of the left half would now be α_0, and the angle of attack of the right half $-\alpha_0$. It is thus clear that the

value of the discontinuity in angle of attack $(\alpha_1 - \alpha_2 = 2\alpha_0)$ is the only factor contributing to the trailing upwash and sidewash in Figure (II). α_1 and α_2 may take on any values within the limitations of the theory.

The methods of calculation are presented in two parts. The first part is the calculation of the upwash in the plane of the wing at 0, 1, 4, and 9 chord lengths behind it. The second part is the calculation of the whole upwash-sidewash field in the Trefftz plane.

B. ANALYTICAL PROCEDURE FOR UPWASH AND SIDEWASH CALCULATIONS.

1. In the plane of the wing at finite distances behind it.

The method used in this part of the calculations is identical to that used in Chapter 7 of reference (1) to evaluate the upwash behind a rectangular wing. The detailed description of the method will not be repeated here. The general procedure is to start with a deflected control surface of infinite span and semi-infinite chord, such as is pictured here. As is described in reference (1), wings of constant differential strength with side edges along t = constant and with leading edges along the line $x_3 = c$, $x_2 = 0$, are superimposed. The strength of these superimposed wings is chosen so that the lift behind $x_3 = c$ due to the original wing is canceled. It is evident that in the limit an infinite number of these wings must be superimposed and their effect summed through integration. The strength of the superimposed wings is determined by the function describing the pressure distribution over the original wing, $u_3 = \frac{2\alpha_0 m U_\infty}{\pi} \cos^{-1}(t)$ from page 9, reference (3). $u_3 = u_3(b)$ is thus $u_3 = \frac{2\alpha_0 m U_\infty}{\pi} \cos^{-1}(b)$. This procedure yields a solution which

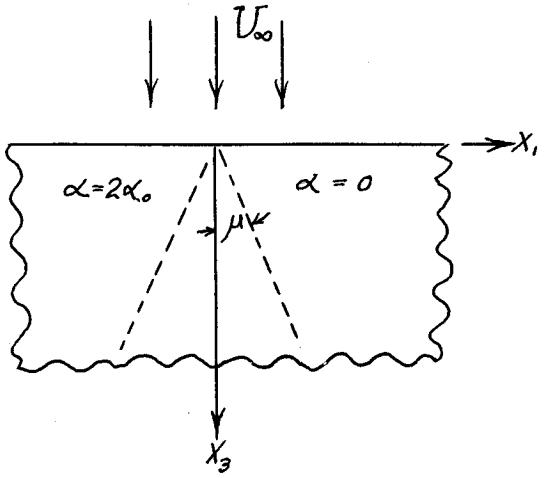

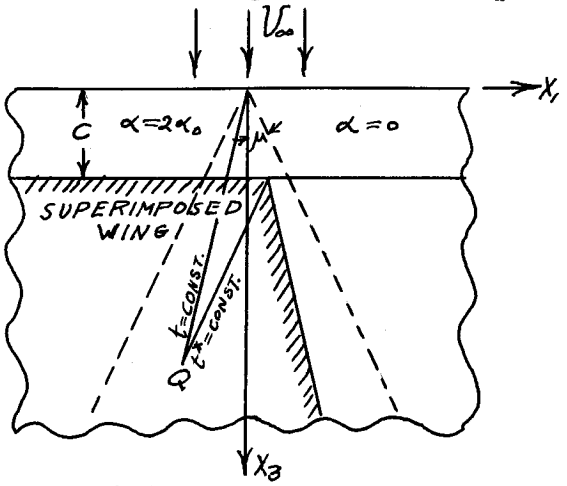

satisfies the boundary conditions for a wing of infinite span and a finite chord, c.

The upwash at any point where $x_3 > c$, $-1 \leq t \leq 1$ is obtained by subtracting the upwash, at that point, due to the superimposed wings, from the upwash, at that point, due to the original wing. The upwash due to the original wing may be expressed as:

$$u_2 = \frac{1}{m}\int_1^{-1} G(b,t)\,\frac{du_3}{db}\,db$$

where from the equation for u_3,

$$\frac{du_3}{db} = -\frac{2\alpha_0 m U_\infty}{\pi}\,\frac{1}{\sqrt{1-b^2}}$$

$$G(b,t) = \frac{1}{\pi}\left(\frac{1}{b}\ln|T| + 2\arctan T + \frac{B^2-1}{2B}\ln\left|\frac{T-B}{1-BT}\right| - \frac{\pi}{2}\right)$$

The upwash due to the superimposed wings may be expressed as:

$$u_2 = \frac{1}{m}\int_1^{-1} G(b,t^*)\,\frac{du_3}{db}\,db$$

where

$$G(b,t^*) = \frac{1}{\pi}\left(\frac{1}{b}\ln|T^*| + 2\arctan T^* + \frac{B^2-1}{2B}\ln\left|\frac{T^*-B}{1-BT^*}\right| - \frac{\pi}{2}\right)$$

Thus the upwash at any point $Q = \left(\frac{x_1}{cm},\ 0,\ \frac{x_3}{c}\right)$ where $\frac{x_3}{c} > 1$, $-1 \leq t \leq 1$ is:

$$u_2 = \frac{1}{m}\int_1^{-1}\left[G(b,t) - G(b,t^*)\right]\frac{du_3}{db}\,db$$

Thus this integral must be evaluated at each point in the wake, where the value of the upwash is to be found.

The integrand in the above expression becomes infinite at certain points in the interval of integration. The

ingenious methods of Lagerstrom and Graham for dealing with these infinities are described below for the three cases encountered in this problem.

CASE I

The function $\left[G(b,t) - G(b,t^*)\right]\frac{du_3}{db}$, hereafter called $\bar{G}(b,Q)\frac{du_3}{db}$, is infinite when $\frac{du_3}{db}$ is infinite, that is, b = ±1, and is infinite when Q lies on the axis of a Mach cone from the tip of a superimposed conical wing as shown in the sketch.

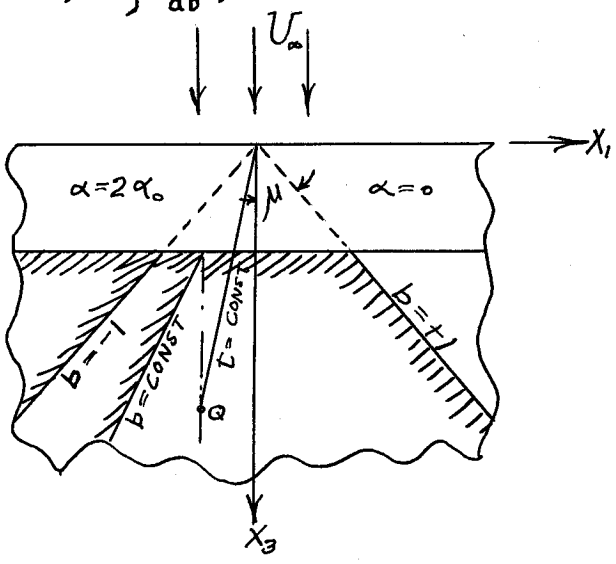

Part A: $\frac{du_3}{db}$ infinity:

The infinity due to $\frac{du_3}{db}$ can be integrated in the following manner:

at b = -1:

$$\int_{b_1}^{-1}\left[\bar{G}(b,Q)\right]\frac{du_3}{db}\,db = \int_{b_1}^{-1}\left[\bar{G}(b,Q) - R\right]\frac{du_3}{db}\,db + \int_{b_1}^{-1} R\,\frac{du_3}{db}\,db$$

where

$$R = \frac{1}{\pi}\left[\ln\left|\frac{T^*}{T}\right| + 2\arctan T - 2\arctan T^*\right]$$

at b = +1:

$$\int_{b_2}^{+1}\left[\bar{G}(b,Q)\right]\frac{du_3}{db}\,db = \int_{b_2}^{+1}\left[\bar{G}(b,Q) - S\right]\frac{du_3}{db}\,db + \int_{b_2}^{+1} S\,\frac{du_3}{db}\,db$$

where

$$S = \frac{1}{\pi}\left[\ln\left|\frac{T}{T^*}\right| + 2\arctan T - 2\arctan T^*\right]$$

Part B: $\bar{G}(b,Q)$ infinity:

For the case when $\bar{G}(b,Q)$ is infinite, that is, when $b = \frac{x_1}{cm}$ ($T^* = 0$), the removal of the infinity is made in the same manner as for the case of a rectangular wing tip as developed in reference (1), in the following manner:

$$\int_{b_3}^{b_4} \bar{G}(b,Q)\frac{du_3}{db}\,db = \int_{b_3}^{b_4}\left[\bar{G}(b,Q)\frac{du_3}{db} - h(b)\right]db + \int_{b_3}^{b_4} h(b)\,db$$

where

$$h(b) = \frac{1}{\pi\frac{x_1}{cm}}\left(\frac{du_3}{db}\right)_{b=\frac{x_1}{cm}}\left[\left(\frac{x_1}{cm}-b\right)\ln\left|\frac{x_1}{cm}-b\right| - \left(\frac{x_1}{cm}-b\right)\right]$$

and

$$\bar{G}(b,Q)\frac{du_3}{db} - h(b) = \left(\frac{du_3}{db}\right)_{b=\frac{x_1}{cm}}\frac{1}{\pi}\left\{\frac{1}{\frac{x_1}{cm}}\left(\ln T + \ln 2\left(\frac{x_3}{c}-1\right)\right)\right.$$

$$\left. + \frac{\sqrt{1-\left(\frac{x_1}{cm}\right)^2}}{\frac{x_1}{cm}}\left[\ln|B| - \ln\left|\frac{T-B}{1-BT}\right|\right] + 2\arctan T\right\}$$

CASE II: $\frac{x_1}{cm} < -1$

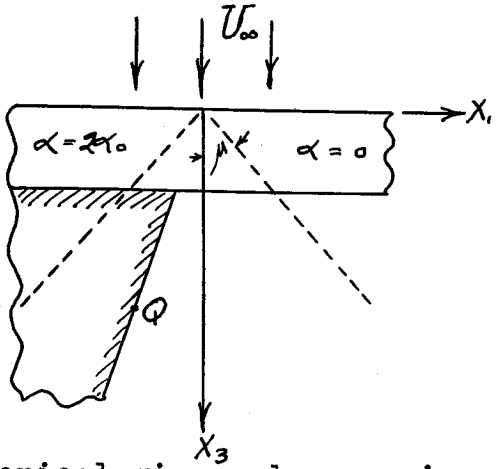

$\bar{G}(b,Q)\frac{du_3}{db}$ is infinite when $\frac{du_3}{db}$ is infinite ($b = \pm 1$) as was shown in Case I. $\bar{G}(b,Q)$ is indeterminate, that is, both $\bar{G}(b,Q)$ and $G(b,t)$ become infinite when $b = t = t^*$. This occurs when Q lies on the edge of a superimposed conical wing and an original wing, each of which produces a line of infinite upwash along its edge. Evaluating $\bar{G}(b,Q)$ at $b = t = t^*$:

$$\bar{G}(b,Q) = \frac{1}{\pi}\left[\frac{1}{b}\ln\left|\frac{T}{T^*}\right| + 2(\arctan T - \arctan T^*) + \frac{B^2-1}{2B}\ln\left|\frac{T-B}{1-BT}\,\frac{1-BT^*}{T^*-B}\right|\right]$$

$$\underset{t=b=t^*}{\bar{G}(b,Q)} = \frac{1}{\pi}\,\frac{B^2-1}{2B}\ln\left|\frac{T-B}{T^*-B}\right|$$

Taking the limit of the argument of the logarithm:

$$\lim_{T\to B}\left(\frac{T-B}{T^*-B}\right)=\frac{d\vec{T}^{\,0}-dB}{dT^*-dB}=\frac{-dB}{dT^*-dB}=\frac{-\frac{dB}{db}}{\frac{dT^*}{dt^*}\frac{dt^*}{db}-\frac{dB}{db}}$$

since

$$\frac{dB}{db}=\frac{B}{b\sqrt{1-b^2}}\quad,\quad\frac{dT^*}{dt^*}=\frac{T^*}{t^*\sqrt{1-t^{*2}}}$$

and

$$\frac{dt^*}{db}=\frac{d}{db}\left(\frac{\frac{x_1}{cm}-b}{\frac{x_3}{c}-1}\right)=\frac{-1}{\frac{x_3}{c}-1}$$

then:

$$\lim_{T\to B}\left(\frac{T-B}{T^*-B}\right)=\frac{-\frac{B}{b\sqrt{1-b^2}}}{\frac{T^*}{t^*\sqrt{1-t^{*2}}}\frac{1}{\frac{x_3}{c}-1}-\frac{B}{b\sqrt{1-b^2}}}=-\frac{\frac{x_3}{c}-1}{\frac{x_3}{c}}$$

hence:

$$\bar{G}(b,Q)_{b=t=t^*=t_b}=\frac{1}{\pi}\frac{\sqrt{1-t_b^2}}{t_b}\ln\left|\frac{\frac{x_3}{c}}{\frac{x_3}{c}-1}\right|$$

CASE III: $\frac{x_1}{cm}=-1$

For this case $\bar{G}(b,Q)\frac{du_3}{db}$ becomes infinite at $b=-1$ due to the infinite upwash along the axis of the Mach cone from the superimposed wing, as in Case I, and because $\frac{du_3}{db}$ becomes infinite at this same point, $b=-1$. Thus we have a double infinity when $b=-1$. In order to subtract out this double infinity, $\bar{G}_s(b,Q)$ and L_s are introduced as follows:

In the interval b_o to -1,

$$\frac{1}{m}\int_{b_o}^{-1}\bar{G}(b,Q)\frac{du_3}{db}\,db\equiv-\frac{2\alpha_o U_\infty}{\pi}\int_{b_o}^{-1}\left[\frac{1}{\sqrt{1-b}}\bar{G}(b,Q)-\frac{1}{\sqrt{2}\,\pi}\ln|1+b|-L_s\right]\frac{db}{\sqrt{1+b}}$$

$$-\frac{2\alpha_o U_\infty}{\sqrt{2}\,\pi^2}\int_{b_o}^{-1}\frac{\ln(1+b)}{\sqrt{1+b}}\,db-\frac{2\alpha_o U_\infty}{\pi}\int_{b_o}^{-1}\frac{L_s}{\sqrt{1+b}}\,db$$

Let:

$$\bar{G}_s(b,Q) = \frac{1}{\sqrt{1+b}}\,\bar{G}(b,Q) - \frac{1}{\sqrt{2}\,\pi}\ln|1+b|$$

and

$$L_s = \bar{G}_s(-1,Q) = \frac{1}{\sqrt{2}\,\pi}\left\{-\ln|T| + 2\arctan T + \lim_{b\to -1}\ln\left|\frac{T^*}{1+b}\right|\right\}$$

as $b\to -1$, $T^*\to\frac{t^*}{2}\to 0$, where $t^* = \dfrac{-1-b}{\frac{x_3}{c}-1}$

$$\lim_{b\to -1}\ln\left|\frac{T^*}{1+b}\right| = \ln\lim_{b\to -1}\left|\frac{\frac{-1-b}{2\left(\frac{x_3}{c}-1\right)}}{1+b}\right| = -\ln\,2\left(\frac{x_3}{c}-1\right)$$

Therefore:

$$L_s = \frac{1}{\sqrt{2}\,\pi}\left\{-\ln|T| + 2\arctan T - \ln 2\left(\frac{x_3}{c}-1\right)\right\}$$

Although $\dfrac{\bar{G}_s(b,Q) - L_s}{\sqrt{1+b}}$ is indeterminate for $b = -1$, it may be shown, by expanding it in a power series, that

$$\lim_{b\to -1}\frac{\bar{G}_s(b,Q) - L_s}{\sqrt{1+b}} = 0$$

Since it is finite for $b = -1$, $-\dfrac{2\alpha_0 U_\infty}{\pi}\displaystyle\int_{b_0}^{-1}\left[\frac{1}{\sqrt{1-b}}\bar{G}(b,Q) - \frac{1}{\sqrt{2}\,\pi}\ln|1+b| - L_s\right]\frac{db}{\sqrt{1+b}}$ is integrated graphically.

$$-\frac{2\alpha_0 U_\infty}{\sqrt{2}\;\pi^2}\int_{b_0}^{-1}\frac{\ln|1+b|}{\sqrt{1+b}}\,db = -.546\,\alpha_0 U_\infty, \quad \text{for } b_0 = -.5$$

$$-\frac{2\alpha_0 U_\infty}{\pi}\int_{b_0}^{-1}\frac{L_s}{\sqrt{1+b}}\,db = (.900)\,\alpha_0 U_\infty L_s, \quad \text{for } b_0 = -.5$$

Now we can write:

$$(u_2)_{\frac{x_1}{cm}=-1} = \frac{1}{m}\int_{1}^{-1} \bar{G}(b,Q)\frac{du_3}{db}\,db \equiv \frac{1}{m}\int_{.5}^{-.5} \bar{G}(b,Q)\frac{du_3}{db}\,db$$

$$-\frac{2\alpha_0 U_\infty}{\pi}\int_{-.5}^{-1}\left[\bar{G}_s(b,Q)-L_s\right]\frac{db}{\sqrt{1+b}} - \frac{2\alpha_0 U_\infty}{\sqrt{2}\,\pi^2}\int_{-.5}^{-1}\frac{\ln|1+b|}{\sqrt{1+b}}\,db - \frac{2\alpha_0 U_\infty}{\pi}\int_{-.5}^{-1}\frac{L_s}{\sqrt{1+b}}\,db$$

$$+\frac{1}{m}\int_{1}^{.5}\left[\bar{G}(b,Q)-S\right]\frac{du_3}{db}\,db + \frac{1}{m}\int_{1}^{.5} S\frac{du_3}{db}\,db$$

where, as before:

$$S=\frac{1}{\pi}\left[\ln\left|\frac{T}{T^*}\right| + 2\arctan T - 2\arctan T^*\right]_{(b=1)}$$

and

$$\frac{1}{m}\int_{1}^{.5} S\frac{du_3}{db} = \frac{2\alpha_0 U_\infty m S}{m\pi}\left[\arccos(b)\right]_{1}^{.5} = .667\,\alpha_0 U_\infty S$$

The first, second and fifth terms of the above expression are integrated graphically.

The upwash immediately behind the trailing edge may be obtained as an analytical function. As before:

$$u_2 = \frac{1}{m}\int_{1}^{-1}\left[G(b,t)-G(b,t^*)\right]\frac{du_3}{db}\,db = -\frac{1}{m}\int_{1}^{-1} G(b,t^*)\frac{du_3}{db}\,db$$

$$+\frac{1}{m}\int_{1}^{0} G(b,t)\frac{du_3}{db}\,db + \frac{1}{m}\int_{0}^{-1} G(b,t)\frac{du_3}{db}\,db$$

From $b = 1$ to $b = 0$, $G(b,t) = 0$, since the original wing was at zero angle of attack here.

From $b = 0$ to $b = -1$, $G(b,t) = -1$ so that:

$$\frac{1}{m}\int_{0}^{-1}(-1)\frac{du_3}{db}\,db = -\left[u_3(-1)-u_3(0)\right] = -2\alpha_0 U_\infty$$

since

$$u_3 = \frac{2\alpha_0 U_\infty m}{\pi} \arccos(t)$$

Likewise:

$$G(b,t^*) = -1$$

giving:

$$\frac{1}{m}\int_1^t \frac{du_3}{db}\,db = \frac{2\alpha_0 U_\infty}{\pi} \arccos(t)$$

The upper limit here is t, since the wings for $b<t$ can not contribute to the upwash at t just behind the trailing edge. Therefore, for $0<t<1$:

$$u_2 = \frac{2\alpha_0 U_\infty}{\pi} \arccos(t)$$

and for $-1<t<0$:

$$u_2 = \frac{2\alpha_0 U_\infty}{\pi} \arccos(t) - 2\alpha_0 U_\infty = -2\alpha_0 U_\infty \left(1 - \frac{1}{\pi}\arccos(t)\right)$$

2. In the Trefftz plane (at $x_3 = \infty$)

The problem of computing the upwash-sidewash field in the Trefftz plane is shown in reference (1) to be the same as that in incompressible flow, and the methods of complex variables may be used.

The vortex sheet trailing back from the wing is unaltered, in the first approximation, from the trailing edge to $x_3 = \infty$, and remains in the plane of the wing. Thus the sidewash is a known function all along the x_1 axis in the Trefftz plane. $u_1 = 0$ for $\frac{x_1}{cm} < -1$ and for $\frac{x_1}{cm} > 1$, since there is no sidewash coming from the two dimensional part

of the wing. Behind the region where the Mach cone intersects the trailing edge of the wing $(-1 \leq \frac{x_1}{cm} \leq 1)$, $u_1 = F(\frac{x_1}{cm})$ at $\frac{x_2}{cm} = 0 + \delta$ and $u_1 = -F(\frac{x_1}{cm})$ at $\frac{x_2}{cm} = 0 - \delta$ where δ is an infinitesimal distance and $\longrightarrow 0$. This furnishes one boundary condition for the problem in the Trefftz plane. The other boundary condition is that u_2 vanish at $r_1 = \sqrt{(\frac{x_2}{cm})^2 + (\frac{x_1}{cm})^2} = \infty$.

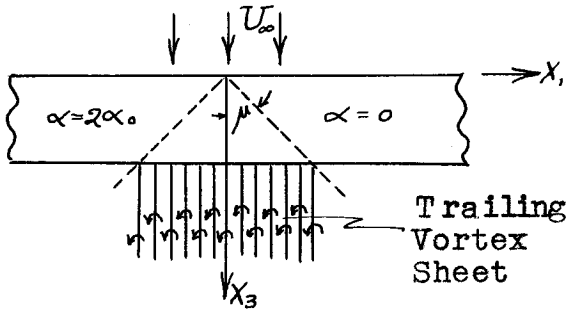

In the Plane of the Wing

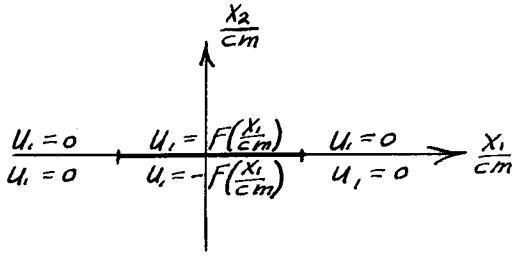

In the Trefftz Plane

The function $F(\frac{x_1}{cm})$ is evaluated at the trailing edge of the wing by use of the well known formula derived from conditions of irrotational flow:

$$\frac{du_1}{dt} = -\frac{1}{mt} \quad \frac{du_3}{dt} \qquad (1)$$

$u_3 = u_3(t)$ is assumed known. For the justification for this procedure, see reference (1).

It was noticed by Dr. Lagerstrom that the same boundary conditions are satisfied when a solution that vanishes on the Mach cone in the $\mathcal{E}$ plane is transformed to the physical (z) plane by the inverted Joukowski transformation:

$$\mathcal{E} = \frac{1 - \sqrt{1 - z^2}}{z}$$

$$\frac{2}{z} = \mathcal{E} + \frac{1}{\mathcal{E}}$$

where $\mathcal{E}$ and z are complex variables.

The $\mathcal{E}$ plane here referred to is that perpendicular to the $\frac{x_3}{c}$ axis at $\frac{x_3}{c} = 1$, and is the one encountered in conical flow problems described in reference (4). In the $\mathcal{E}$ plane, the coordinates have been transformed from the physical plane through the Chaplygin transformation $R = \frac{1-\sqrt{1-r_1^2}}{r_1}$ to allow the use of the solutions to Laplace's equation.

It may be seen that in applying the inverted Joukowski transformation, the unit circle in the $\mathcal{E}$ plane transforms into the portion of the x_1 axis in the physical plane where $|x_1| \geq 1$. It is also seen that the point $R = 1$, $\theta = \frac{\pi}{2}$ in the $\mathcal{E}$ plane transforms to $\frac{x_1}{cm} = \infty$ in the physical plane. Thus the boundary conditions in the $\mathcal{E}$ plane for $u_1 - iu_2 = U_{(\mathcal{E})}$ become $u_1 = 0$ on the unit circle, $u_2 = 0$ at $R = 1$, $\theta = \frac{\pi}{2}$ and $U(x) = F(\frac{x_1}{cm})$ on the x axis, where, by the Chaplygin transformation:

$$X = \frac{1-\sqrt{1-(\frac{x_1}{cm})^2}}{(\frac{x_1}{cm})} \qquad (2)$$

Now the procedure outlined above will be applied to the problem at hand. From reference (3):

$$u_3 = \frac{2\alpha_0 m U_\infty}{\pi} \cos^{-1}(+t)$$

and by formula (1):

$$u_1 = \frac{-2\alpha_0 U_\infty}{\pi} \ln\left|\frac{1+\sqrt{1-t^2}}{t}\right|$$

At the trailing edge $t = \frac{x_1}{cm}$, therefore:

$$u_1 = \frac{2\alpha_0 U_\infty}{\pi} \ln\left|\frac{1-\sqrt{1-(\frac{x_1}{cm})^2}}{\frac{x_1}{cm}}\right| = F(\frac{x_1}{cm})$$

Now using formula (2) in the $\mathcal{E}$ plane:

$$u_1 = \frac{2\alpha_0 U_\infty}{\pi} \ln(x)$$

The boundary conditions on u_1 are obviously satisfied for:

$$u_1 - iu_2 = \frac{2\alpha_0 U_\infty}{\pi}\left[\ln(\mathcal{E}) - i\frac{\pi}{2}\right]$$

$$u_1 = \frac{2\alpha_0 U_\infty}{\pi} \ln r$$

$$u_2 = \frac{2\alpha_0 U_\infty}{\pi}\left(\frac{\pi}{2} - \theta\right)$$

Thus in the $\mathcal{E}$ plane, R = constant represents lines of constant sidewash, and θ = constant represents lines of constant upwash.

It is easiest to think of the transformation $\frac{1}{z} = \frac{1}{2}\left(\mathcal{E} + \frac{1}{\mathcal{E}}\right)$ in two steps: $\frac{1}{2}\left(\mathcal{E} + \frac{1}{\mathcal{E}}\right) = \mathcal{E}_1$ and $\mathcal{E}_1 = \frac{1}{z}$. The first step is the well known Joukowski transformation, and the second is the ordinary inversion about the unit circle. From this, the formulas for the lines of constant sidewash and upwash in the physical plane turn out to be:

$$r_1^2 = \left[\frac{(2c_3)^2}{(c_3^2-1)^2}\sin^2\theta_1 + 1\right]\frac{(2c_3)^2}{(c_3^2+1)^2}$$

where: $c_3 = e^{\frac{\pi}{2}\frac{u_1}{\alpha_0 U_\infty}}$

r_1 and θ_1 are the polar coordinates in the z (physical) plane.

$$r_1^2 = \frac{(1-c_1^2) - \sin^2\theta_1}{(1-c_1^2)\,c_1^2}$$

where: $c_1 = \cos\left[\left(1 - \frac{u_2}{\alpha_0 U_\infty}\right)\frac{\pi}{2}\right]$

These are plotted in Figures (V) and (VI). Figures (VII) and (VIII) are crossplotted from Figures (V) and (VI).

C. RESULTS AND DISCUSSION

Figure (III) presents the data for upwash in the plane of the wing at 0, 1, 4, and 9 chord lengths behind the trailing edge of a deflected control surface of infinite span. The method of calculating the points on this plot was that described in Part B-1. It is noted that downwash is found in the wake of the section of the control surface at the greater angle of attack. Similarly, upwash is associated with the surface at the smaller angle of attack. Since the plot is symmetrical with respect to the origin, there is no net upwash. It may be seen that this must be the case by studying the symmetry properties of the problem. The pressure distribution on the wing (as shown in the sketch ($c_p = -\frac{2u_3}{U_\infty}$)) in region III, Figure (I), is antisymmetric with respect to the x_2, x_3 plane. The strength of the compression or expansion wave at the trailing edge is determined by the pressure change across the wave which is necessary to equalize the pressure in the flow behind the top and bottom of the wing, and to make these flows vertically parallel. Thus it is clear that, to the first approximation, the pressure distribution on the wing determines the strength of the shock or expansion wave at the trailing edge. The strength of these waves at the trailing

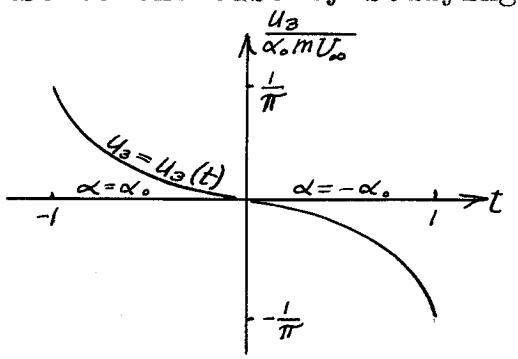

Pressure Distribution on the Wing Inside Mach Cone III of Figure (I).

edge in turn determines the vertical angle through which the flow passing over the wing is turned as it passes by the trailing edge. On the top of the wing $u_2 = -\alpha_0 U_\infty$ in section IIIa, and $u_2 = +\alpha_0 U_\infty$ in section IIIb, and is thus also antisymmetric with respect to the x_2, x_3 plane. Now, since both the upwash on the wing and the strength of the wave at the trailing edge are antisymmetric with respect to the x_2, x_3 plane, the upwash directly behind the trailing edge must be antisymmetric with respect to the x_2, x_3 plane. It is easy to show that the upwash field must continue to be antisymmetric in this way as the flow continues downstream. Consider wing I in the sketch. At point (a, o, b) in the wake, the upwash is equal to n'. At the image of this point in the x_2, x_3 plane, point (-a, o, b), the upwash is equal to m'. Now consider wing II, where the angle of attack distribution has been reversed. The values of the upwash at the same points considered above will be reversed. In a flow described by superimposing wing I on wing II, there will be no disturbances, since this results in a flat plate at zero angle of attack. Therefore, adding the upwashes at the

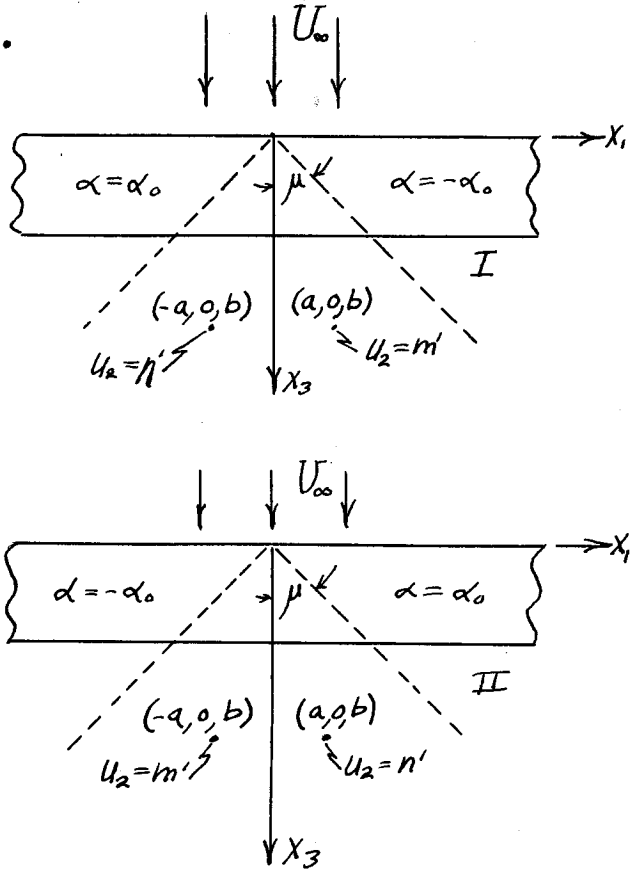

point (a, o, b) in the flow for the flat plate at zero angle of attack, gives $m' + n' = 0$, or $m' = -n'$. Thus the upwash field is antisymmetric with respect to the x_2, x_3 plane everywhere in the flow. By a similar argument, the sidewash may be shown to be symmetric with respect to the x_2, x_3 plane.

The break in the curve where the upwash becomes nearly constant as one approaches the origin from either side in the flow of the wing is directly behind the point where the Mach cone intersects the trailing edges of the control surface.

Figure (IV) shows the lines of constant upwash in the plane of the wing behind a deflected control surface of infinite span. The data in this Figure, at finite distances behind the wing, were obtained by cross-plotting Figure (III). The data at infinity were obtained by cross-plotting the upwash, in the plane of the wing, from Figure (VII). This plot clearly shows that the solution for the upwash at finite distances behind the wing approaches the solution in the Trefftz plane satisfactorily. From this Figure, it is seen that the distribution of upwash at about four chord lengths behind the wing is very nearly the same as that in the Trefftz plane in the range $-2 \leqslant \frac{x_1}{cm} \leqslant 2$. It follows then, that the distribution of upwash and sidewash in the plane perpendicular to the x_3 axis at $\frac{x_3}{c} \geqslant 5$ is very nearly the same as in the Trefftz plane, especially in the vicinity of the x_3 axis.

Figure (V) shows the upwash-sidewash field in the Trefftz

plane for a wing made up of a deflected control surface of infinite span. The data for this Figure were calculated by the method described in Part B-2. The lines of constant upwash and sidewash are described by formulas of that part. The upwash has a maximum positive value equal to that in section IV of Figure (I). This value extends from $\frac{x_1}{cm} = 0$ to $\frac{x_1}{cm} = 1$ in the plane of the wing. The maximum downwash (negative upwash) has the same absolute value and extends from $\frac{x_1}{cm} = 0$ to $\frac{x_1}{cm} = -1$. The upwash is zero along the x_2 axis and at infinity. The curves of constant upwash are modified lemniscates with $\frac{u_2}{\alpha_0 U_\infty}$ positive in the first and fourth quadrants, and negative in the second and third quadrants. Thus upwash is symmetrical with respect to the $\frac{x_1}{cm}$ axis, and antisymmetrical with respect to the $\frac{x_2}{cm}$ axis.

The sidewash has a logarithmic singularity at the origin. It is zero along the $\frac{x_1}{cm}$ axis for $\left|\frac{x_1}{cm}\right| > 1$ and at infinity. The curves of constant sidewash are orthogonal to the curves of constant upwash. The values of the sidewash are symmetrical with respect to the $\frac{x_2}{cm}$ axis, and antisymmetrical with respect to the $\frac{x_1}{cm}$ axis.

Figure (VI) presents the curves of constant upwash and sidewash in the first quadrant of the Trefftz plane, plotted to a larger scale, with the addition of more curves of constant upwash to make interpolation easier. This Figure is meant to furnish an accurate plot from which the value of the sidewash or upwash at any point in its extent may be determined.

The data from Figure (VI) have been cross-plotted in

Figures (VII) and (VIII). Figure (VII) shows the variation of upwash with $\frac{x_1}{cm}$ at $\frac{x_2}{cm} = 0, \pm.5$, and ± 1.0. Figure (VIII) shows the variation of sidewash with $\frac{x_2}{cm}$ at $\frac{x_1}{cm} = 0, \pm.5$, and ± 1.0. These two graphs show clearly that adverse induced rolling moments are experienced by both the horizontal and vertical aerodynamic surfaces placed in the wake of a deflected control surface of infinite span. The upwash on the horizontal tail gives it an effective angle of attack which is opposite in sign to that of the roll control surface. The exact value of the induced rolling moment depends on the chord of the rear aerodynamic surface and its span. The induced angle of attack varies across the span of the rear aerodynamic surface. The exact value of the induced rolling moment would have to be calculated using a method which gives the distribution of pressure over a wing with any arbitrary aerodynamic twist.

Figure (IX) shows the very simple case of a canard configuration whose roll control surface has an effective aspect ratio of 2.0, and whose wing has a chord equal to, or greater than, and a span equal to that of the roll control surface. This configuration is for illustration, and no vertical surfaces are considered here. The accompanying graph shows the upwash distribution on the wing. The upwash due to the tips on the roll control surface (reference 1) is superimposed on the upwash due to the discontinuity of angle of attack to get the final distribution. Since $\left|\frac{u_2}{\alpha_0 U_\infty}\right| \geq 1$ all along the span on the rear wing, the induced rolling moment is such that strong roll reversal would be encountered.

A vertical tail symmetrical about the x_1, x_3 plane would have a similarly induced adverse rolling moment. If the tail were not symmetrical with respect to the x_1, x_3 plane, a yawing moment would also be induced.

Viscosity effects would modify the upwash-sidewash distribution somewhat, particularly in the immediate vicinity of the origin, where the discontinuities in both upwash and sidewash would be smoothed out. It is believed that the essential features of these induced trailing velocities would not be altered.

The values of the induced velocities in this analysis are a whole order of magnitude higher than those encountered in subsonic flow. Therefore, if it were possible to calculate the second order effect of having the free vortices which trail back from the wing follow the streamlines of the flow calculated in this paper, rather than the free stream direction, the upwash-sidewash field could conceivably be altered to a considerable extent.

Reliable experimental data are urgently needed to check the assumptions made in the theory used to obtain the results presented in this report.

LIST OF REFERENCES

1. Lagerstrom, Paco A.; Graham, Martha E.; "Downwash and Sidewash Induced by Three-Dimensional Lifting Wings in Supersonic Flow"; Douglas Report SM - 13007; (April, 1947).

2. Kahane, A.; Lees, Lester; "The Flow at the Rear of a Two-Dimensional Supersonic Airfoil"; Journal of the Aeronautical Sciences; (March, 1948); Volume 15, Number 3.

3. Lagerstrom, Paco A.; Graham, Martha E.; "Linearized Theory of Supersonic Control Surfaces"; Douglas Report SM - 13060; (July, 1947).

4. Lagerstrom, Paco A.; J. P. L. Progress Report; Number 4-36.

5. Stewart, Homer J.; "The Lift of a Delta Wing at Supersonic Speeds"; Quarterly of Applied Mathematics; (October, 1946); Volume IV, Number 3.

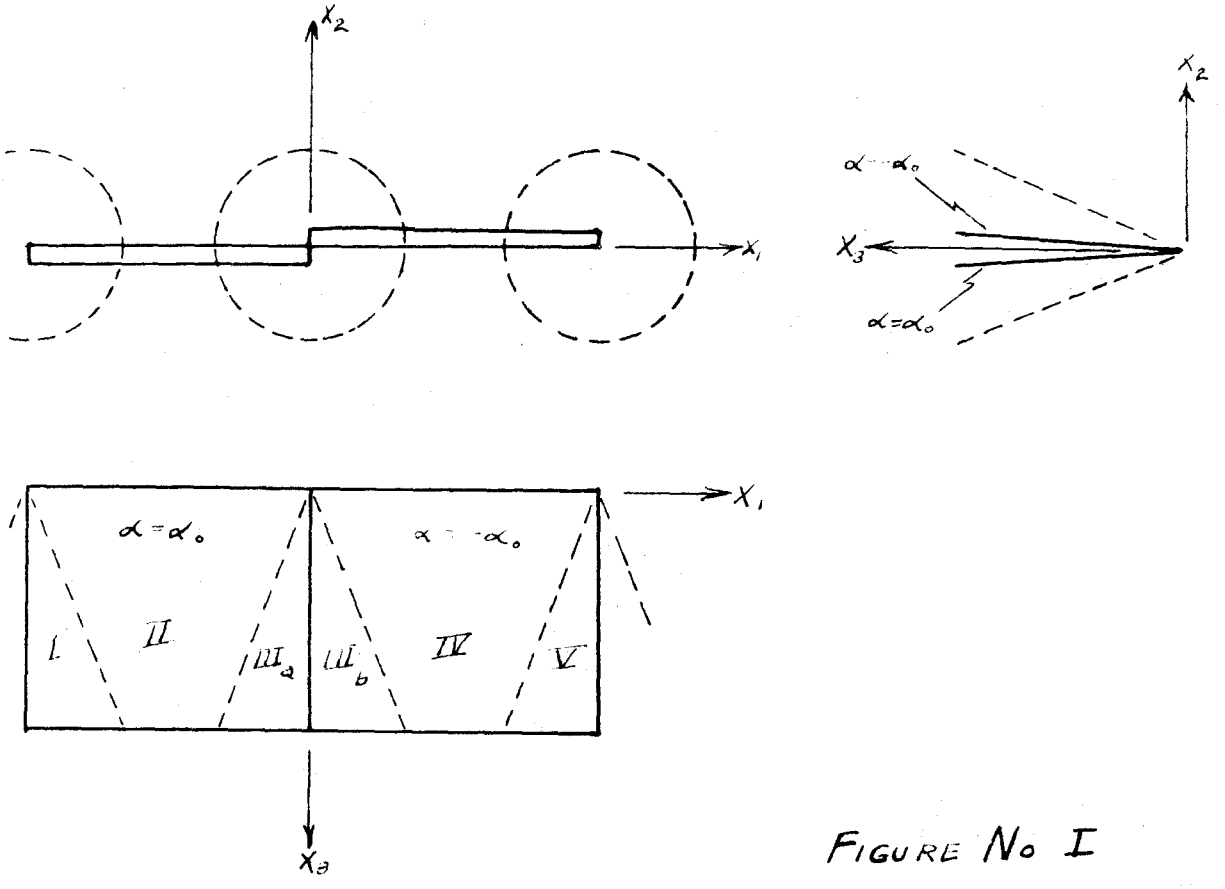

FIGURE No I

EXAMPLE OF A CANARD TYPE ROLL CONTROL SURFACE

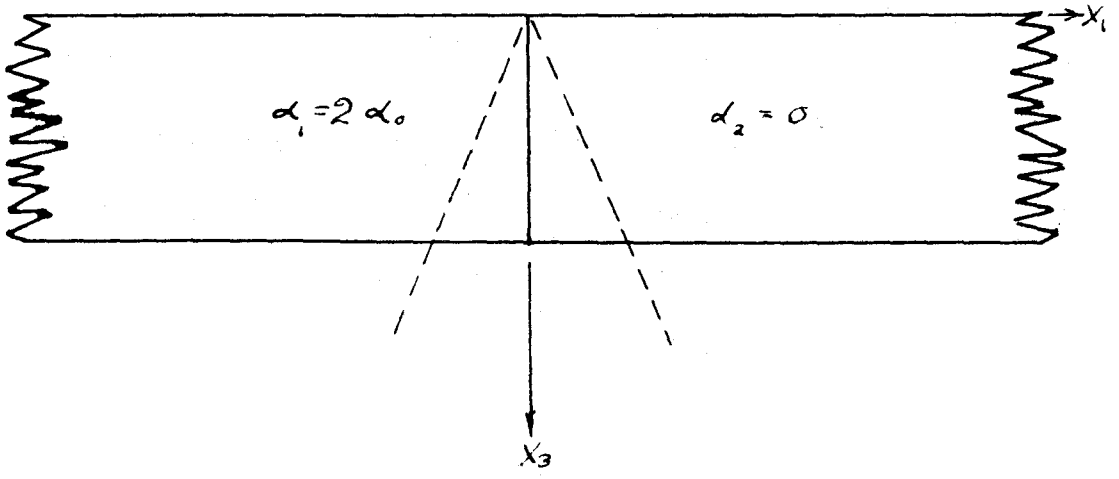

FIGURE No. II

ROLL CONTROL SURFACE WITH INFINITE SPAN

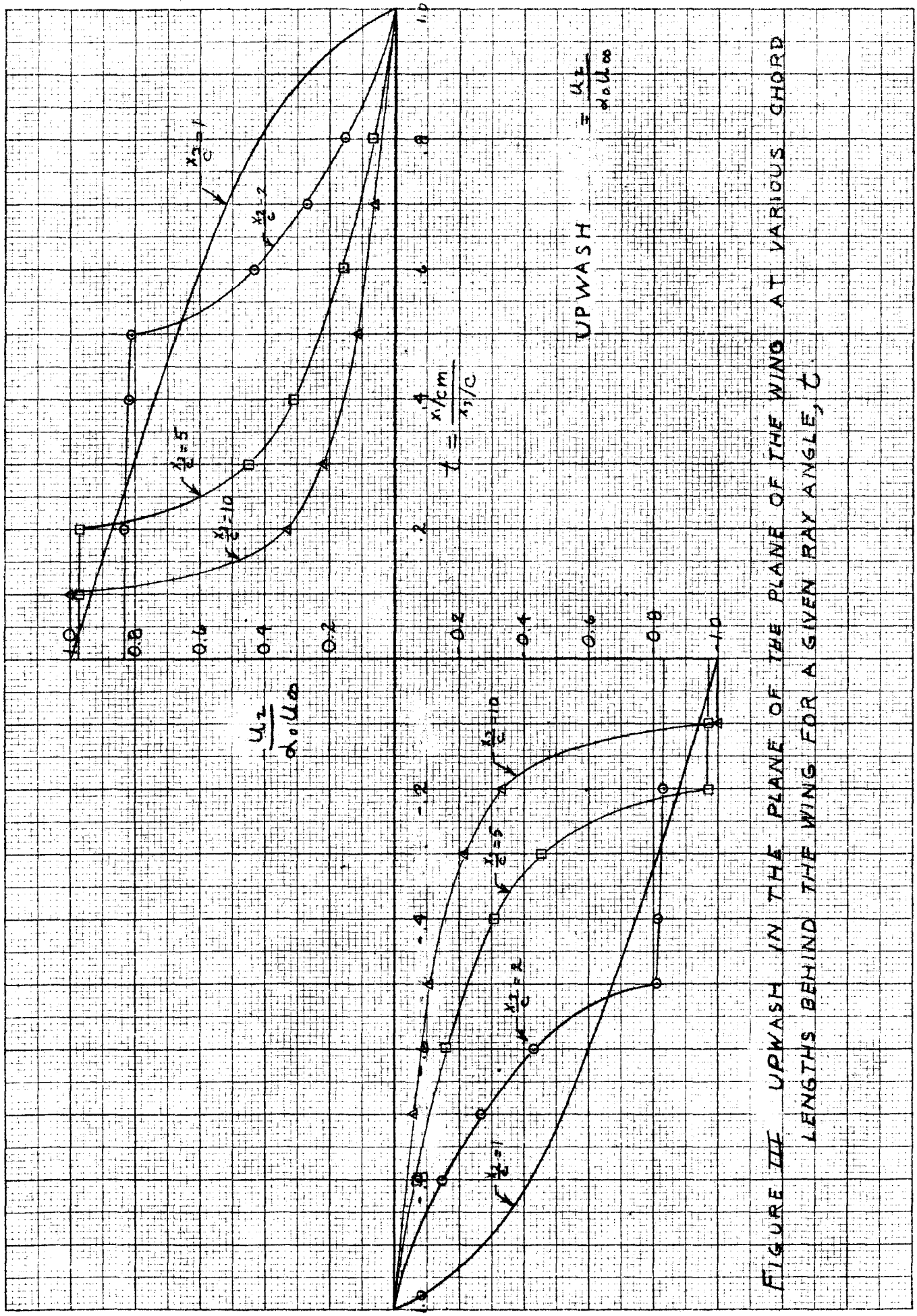

FIGURE III UPWASH IN THE PLANE OF THE WING AT VARIOUS CHORD LENGTHS BEHIND THE WING FOR A GIVEN RAY ANGLE, ζ

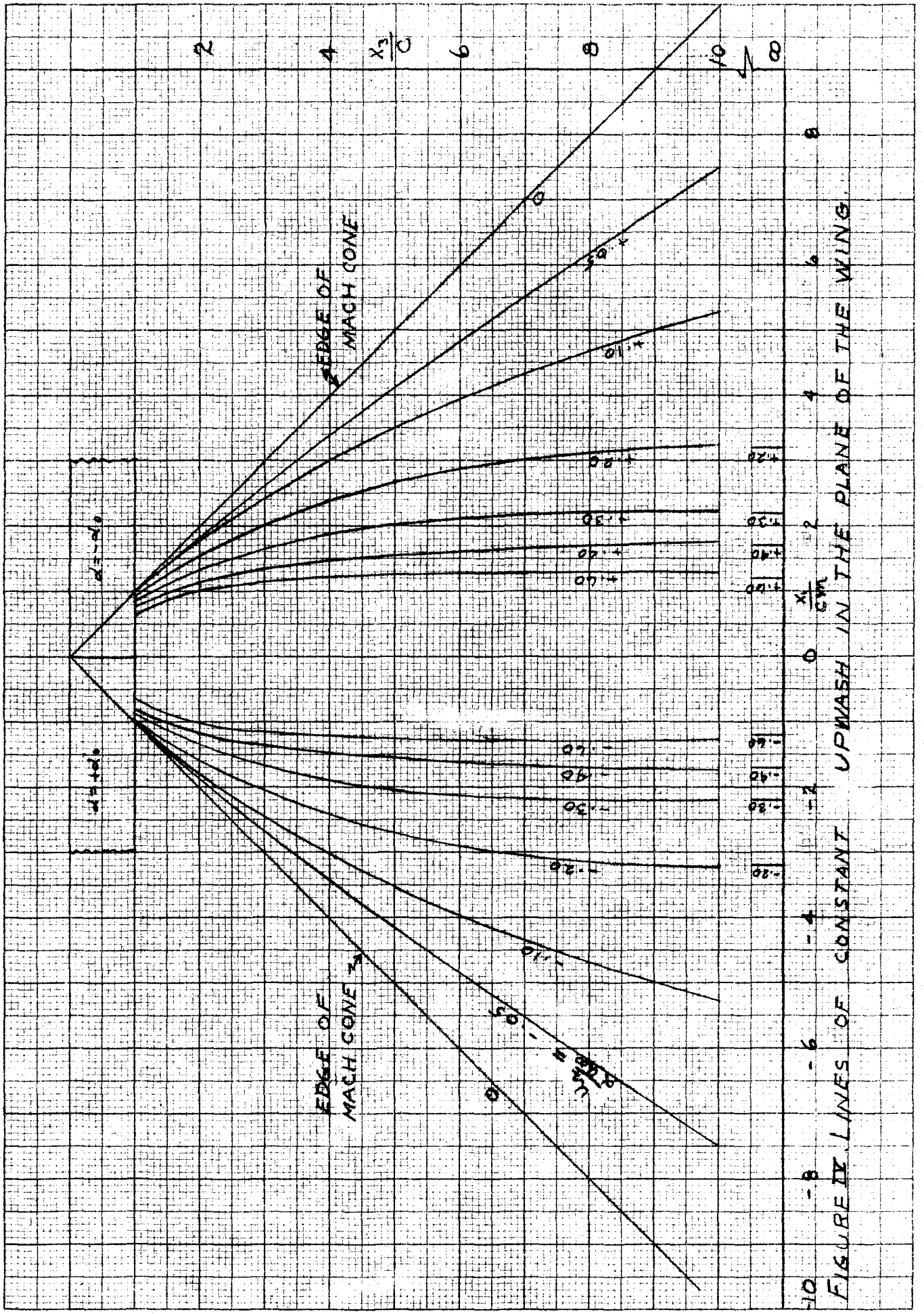

FIGURE IV. LINES OF CONSTANT UPWASH IN THE PLANE OF THE WING

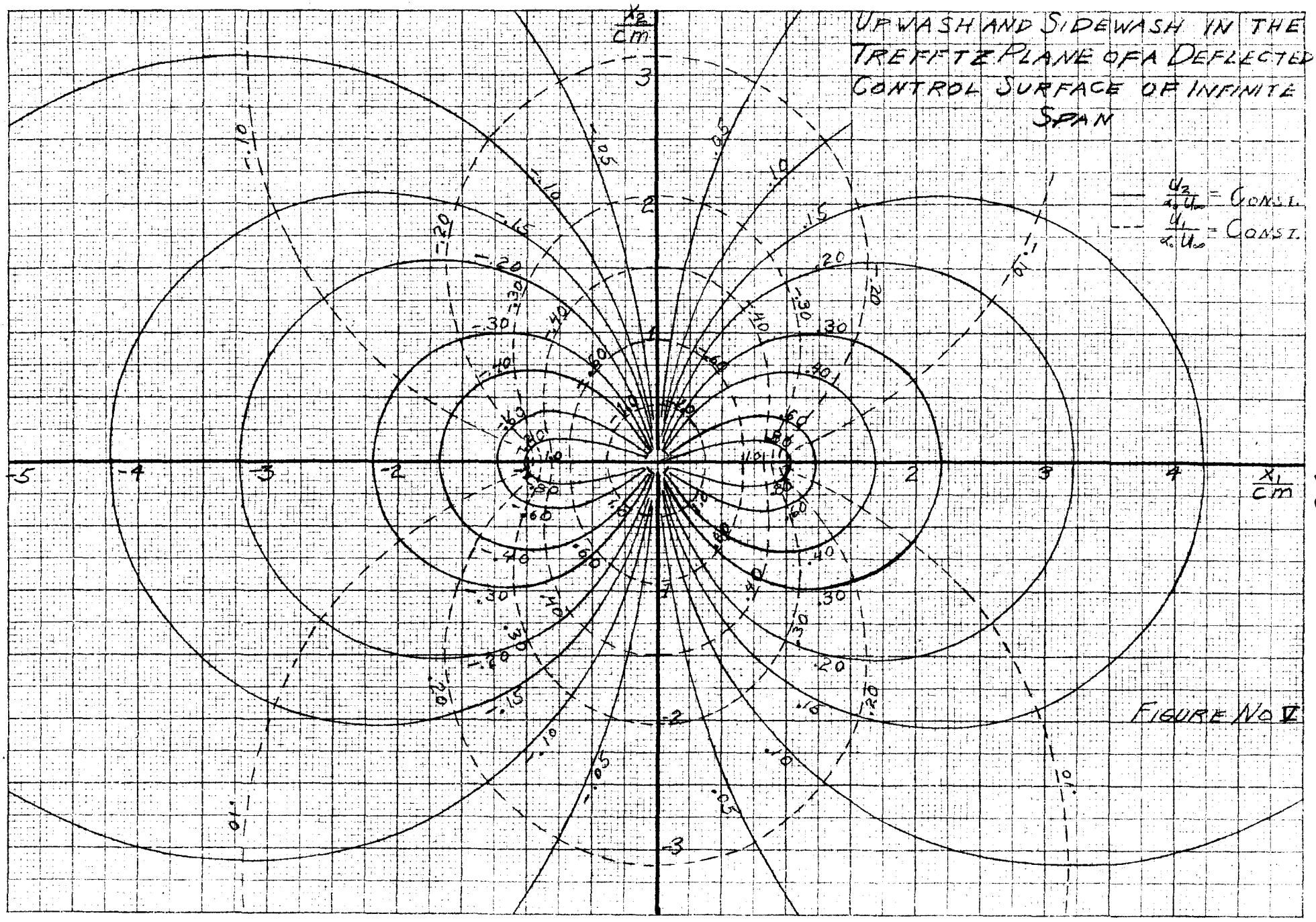
UPWASH AND SIDEWASH IN THE TREFFTZ PLANE OF A DEFLECTED CONTROL SURFACE OF INFINITE SPAN
$\frac{u_2}{\alpha U_\infty}$ = CONST.
$\frac{u_1}{\alpha U_\infty}$ = CONST.
$\frac{x_2}{cm}$
$\frac{x_1}{cm}$

FIGURE NO V

UPWASH & SIDEWASH IN THE FIRST QUADRANT OF THE TREFFTZ PLANE OF A DEFLECTED CONTROL SURFACE OF INFINITE SPAN

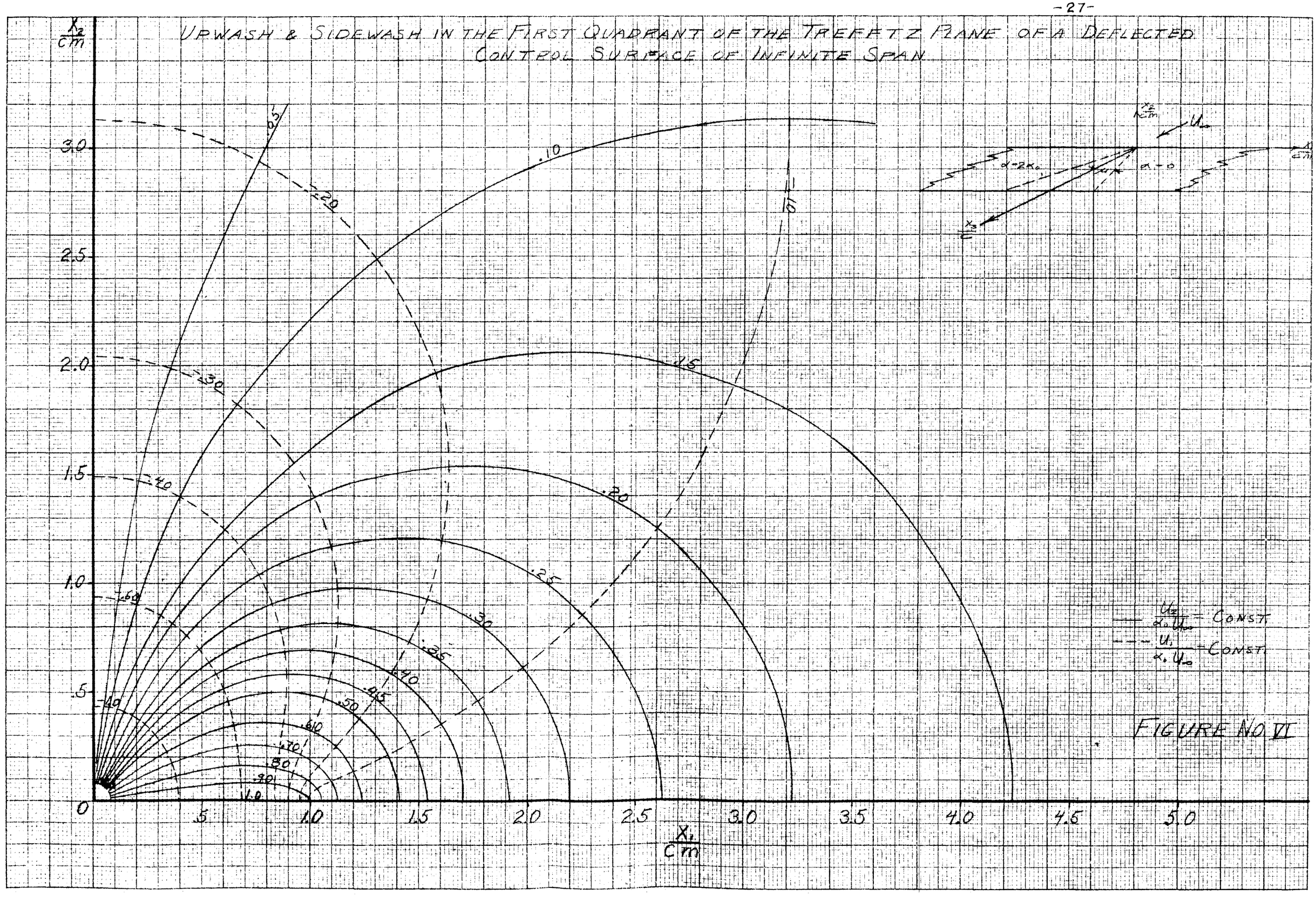

FIGURE NO VI

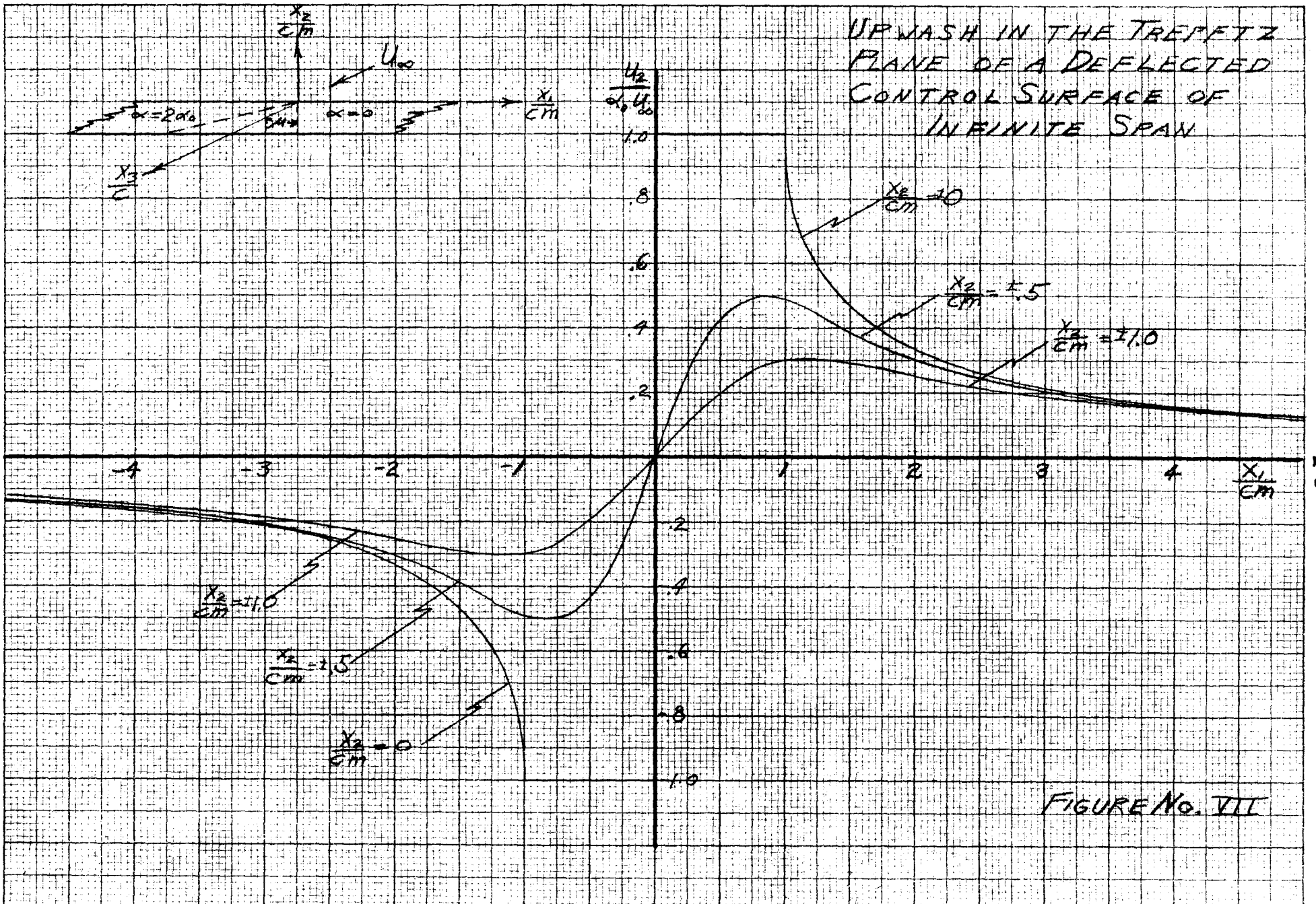

FIGURE NO. VII

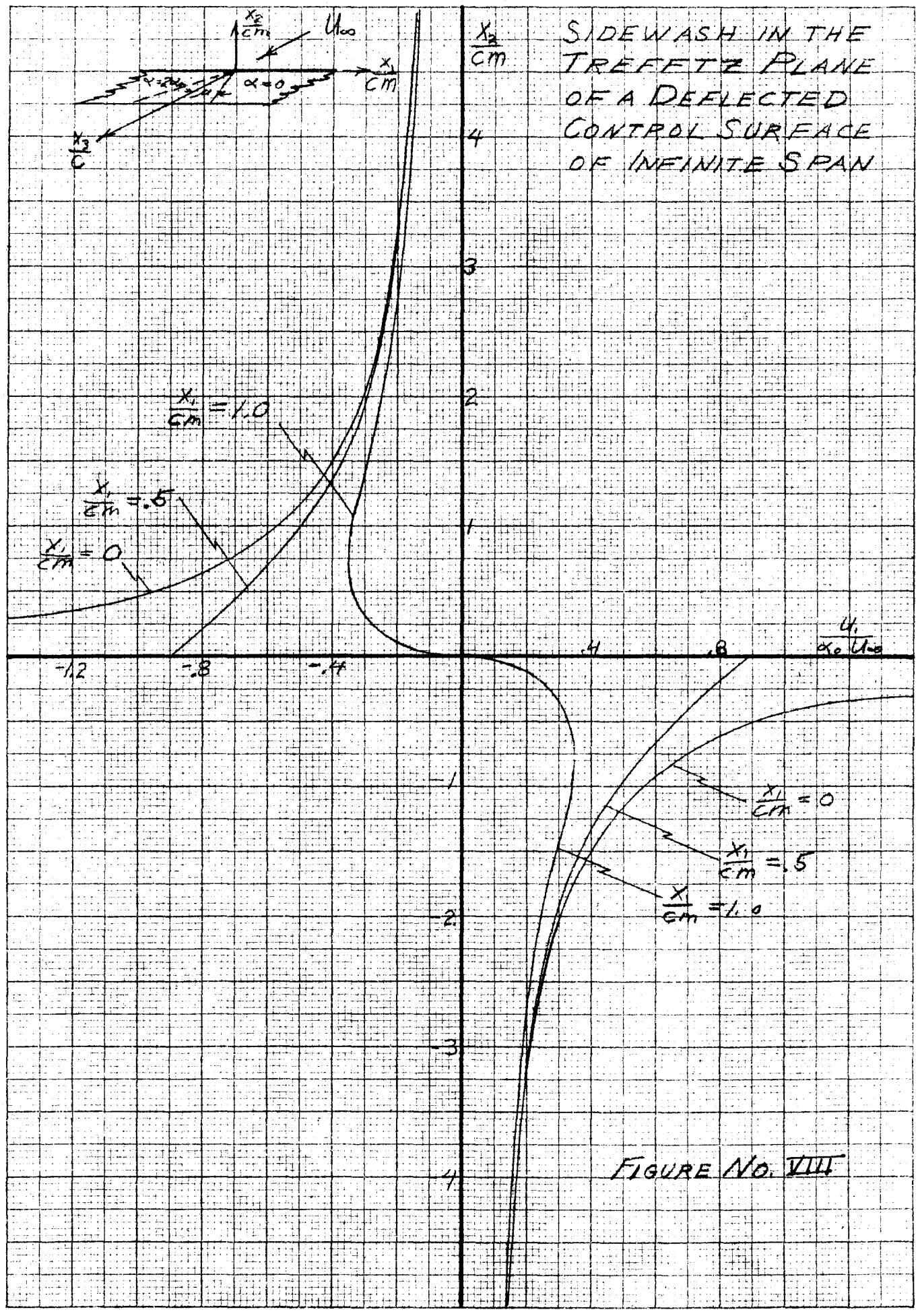

FIGURE NO. VIII

ILLUSTRATION OF ONE POSSIBILITY FOR OBTAINING ROLL REVERSAL.

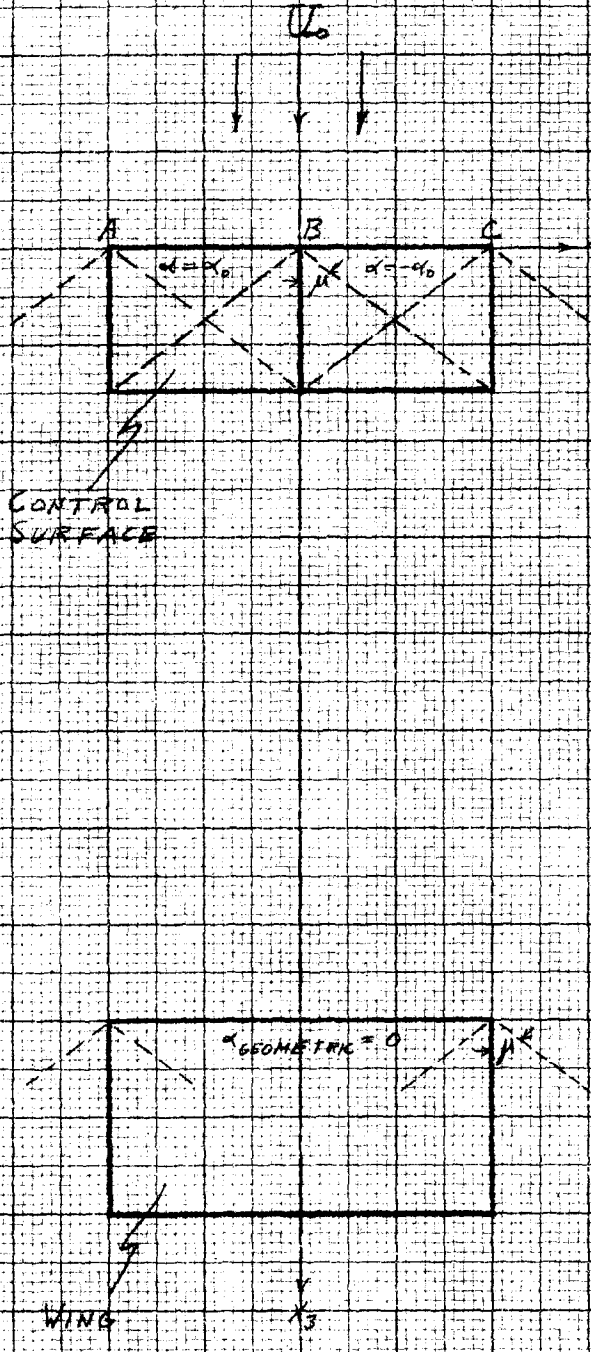

SIMPLIFIED CANARD CONFIGURATION

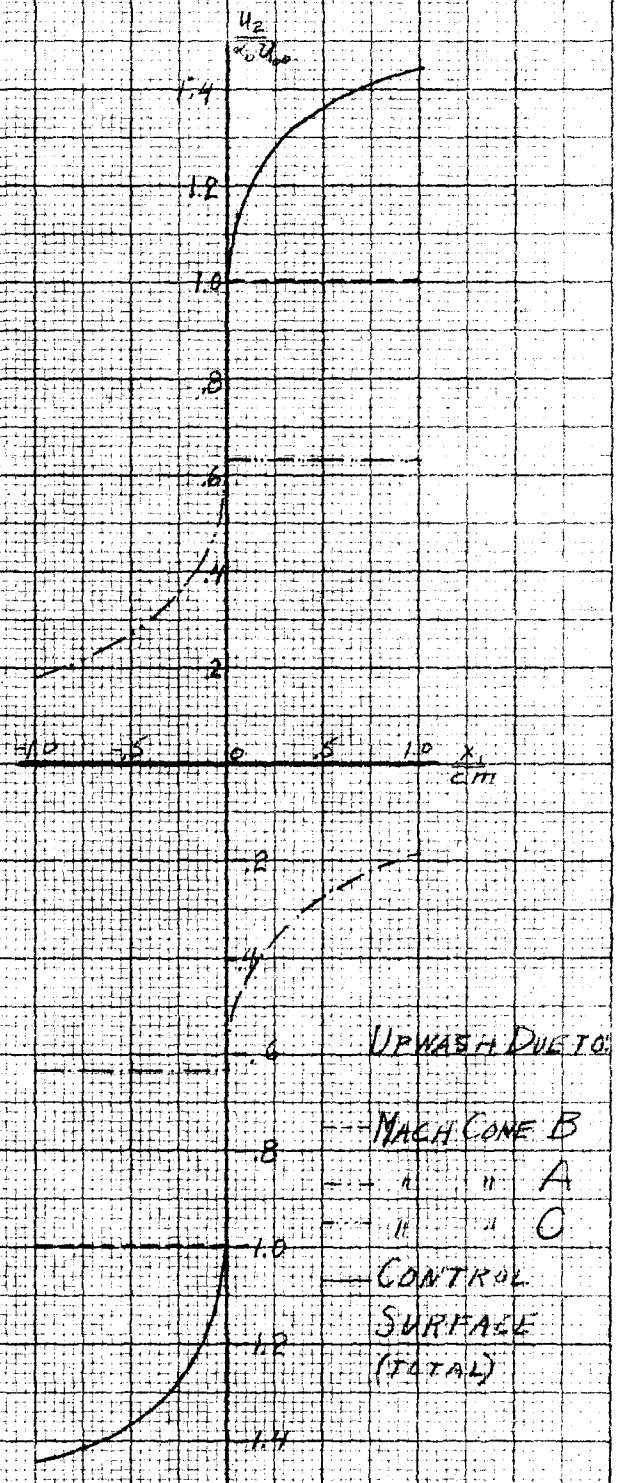

UPWASH DISTRIBUTION AT LEADING EDGE OF CANARD WING.

FIG. NO. IX